Metabolic Engineering 91 (2025) 44–58

Contents lists available at ScienceDirect

Metabolic Engineering

journal homepage: www.elsevier.com/locate/meteng

Enhancing oil feedstock utilization for high-yield low-carbon polyhydroxyalkanoates industrial bioproduction

Tianyu Jiang [a,1], Tingting Tan [a,1], Zhiyuan Zong [b], Dingding Fan [a], Jianxin Wang [a], Yanci Qiu [a], Xin Teng [a,*], Haoqian M. Zhang [a,**], Chitong Rao [a,***]

[a] Bluepha Co. Ltd., Shanghai, China
[b] Department of Engineering Science, University of Oxford, Oxford, OX1 3PJ, UK

ARTICLE INFO

Keywords:
Polyhydroxyalkanoates
Cupriavidus necator
Oil consumption
Industrial scalability
Unbiased screening

ABSTRACT

Polyhydroxyalkanoates (PHAs) are biodegradable and environmentally sustainable alternatives to conventional plastics, yet their adoption has been hindered by the high production costs and scalability challenges. This study employed unbiased genomics approaches to engineer *Cupriavidus necator H16, an industrial* strain with intrinsic capabilities for PHA biosynthesis, for enhanced utilization of oil-based feedstocks, including food-grade palm oil and crude waste cooking oil. The engineered strain demonstrated significant improvements in PHA production, achieving a 264 g/L yield (25.4 % increase) and a 100 g/g conversion rate of palm oil (12 % increase) in 60-h fed-batch fermentation at 150 m^3 production scale, the highest yield and conversion rate using food-grade palm oil as carbon source reported to the best of our knowledge. Notably, the carbon footprint of PHA production was reduced by 29.7 % using the engineered strain, and could be further reduced by adopting waste cooking oil. Mechanistic studies revealed that the *H16_A3043/H16_A3044* two-component system plays a central role in regulating stress response and biogenesis, the deletion of which unlocked the regulatory constraint and enhanced oil feedstock consumption. This mutation, supplemented with the necessary lipase engineering as revealed during the scale-up troubleshooting, confered higher PHA production in a robust fermentation process scalable through 0.5 L, 200 L, 15 m^3 and 150 m^3. Additionally, the engineered strain demonstrated efficient utilization of waste cooking oil for PHA production. This study bridges laboratory-scale advancements and industrial feasibility, demonstrating a scalable, sustainable, and economically viable pathway for biopolymer production, contributing to the global shift toward a circular bioeconomy.

1. Introduction

Polyhydroxyalkanoates (PHAs) are a group of biodegradable polyesters produced by various microorganisms as intracellular carbon and energy reserves. As renewable, biodegradable polymers, PHAs have attracted significant attention due to their potential to replace conventional petrochemical-based plastics (Park et al., 2024). Their biodegradability makes PHA an environmentally friendly alternative, as PHA materials break down in natural environments without leaving harmful long-term residues. These properties have led to growing interest in their applications across multiple industries, including bioplastics, agriculture, and medicine (Park et al., 2024). By contributing to waste reduction and environmental sustainability, PHAs offer a promising solution to the global plastic waste crisis. As concerns over the environmental impact of petroleum-based plastics continue to grow, developing green and sustainable production methods for biopolymers like PHA has become a global priority.

The production of PHA relies heavily on the choice of carbon source, which plays a critical role in determining both the structure and yield of the polymer (Saravanan et al., 2022). Traditionally, simple sugars such as glucose, sucrose, and starch have been used as primary carbon sources for PHA production (Dietrich et al., 2019). However, the high cost of these substrates and their competition with the food industry present significant barriers to large-scale PHA manufacturing (Jiang et al., 2016;

* Corresponding author. No. 210, Lane 345, Guangyue Road, Hongkou District, Shanghai, China.
** Corresponding author. No. 210, Lane 345, Guangyue Road, Hongkou District, Shanghai, China.
*** Corresponding author. No. 210, Lane 345, Guangyue Road, Hongkou District, Shanghai, China.
E-mail addresses: tengxin@bluepha.com (X. Teng), zhanghaoqian@bluepha.com (H.M. Zhang), raochitong@gmail.com (C. Rao).
[1] These authors contributed equally to this work.

https://doi.org/10.1016/j.ymben.2025.04.001
Received 27 January 2025; Received in revised form 3 April 2025; Accepted 4 April 2025
Available online 4 April 2025
1096-7176/© 2025 International Metabolic Engineering Society. Published by Elsevier Inc. All rights are reserved, including those for text and data mining, AI training, and similar technologies.

Koller and Braunegg, 2018; Yañez et al., 2020). In fact, carbon substrates can constitute up to 50 % of the total production cost (Braunegg et al., 2004), making PHA more expensive than conventional petroleum-based plastics (Lim et al., 2023; Park et al., 2024). In response to these challenges, researchers have explored alternative, cost-effective carbon sources for PHA production, including plant oils (Ng et al., 2010), food wastes (Ruiz et al., 2019; Nielsen et al., 2017), and agricultural by-products (Dietrich et al., 2019). Among these, plant oils, particularly palm oil, stand out as promising options due to their high carbon content, low cost, consistent quality and wide availability (Chien Bong et al., 2021). These oils are rich in fatty acids, which can be converted into acyl-CoA derivatives that feed into the PHA biosynthesis pathways. Additionally, waste oils like waste cooking oil (WCO) offer an even more economical alternative by recycling discarded materials into valuable biopolymers, thus supporting environmental sustainability by aligning with circular economy principles.

Reducing PHA production costs can be achieved by combining high-efficiency production strains with cost-effective feedstocks. Carbon source utilization efficiency is a critical factor for industrial production, as it directly impacts both the economic viability and sustainability of the process. Advances in genetic engineering and metabolic pathway optimization have enabled researchers to improve the conversion of diverse carbon sources into high PHA yields (Wang et al., 2023). For instance, the heterologous expression of xylose isomerase and xylulokinase in *Cupriavidus necator* and *Pseudomonas putida* has allowed these strains to efficiently utilize xylose, the second most abundant sugar in lignocellulose, as a feedstock (Le Meur et al., 2012; Kim et al., 2016). Similarly, the heterologous expression of β-glucosidase in *P. putida* has enabled the strain to grow on cellobiose, a major component of food waste, as the sole carbon source (Dvořák and de Lorenzo, 2018). While significant progress has been made in optimizing carbohydrate-based feedstocks, comparatively fewer studies have investigated oil-based substrates. Although promising results have been reported in *Escherichia coli* (Park et al., 2005), research on industrially relevant production chassis, such as *C. necator*, remains limited. Leveraging strains with high carbon utilization efficiency for oil-based substrates could unlock new opportunities for cost-effective and sustainable PHA production at scale.

C. necator H16 is one of the most extensively studied PHA-producing bacteria (Reinecke and Steinbüchel, 2009). Known for its ability to accumulate polyhydroxybutyrate (PHB) up to 72 %–76 % of its dry cell weight (DCW) when grown on soybean oil (Kahar et al., 2004), *C. necator* has been adopted as the production strain by leading PHA manufacturers, including Bluepha, Kaneka, Danimer Scientific, and Tianan Biologic. In many industrial applications such as antibiotics and biomaterials, production strains are selected from naturally occurring wild-type strains that exhibit strong intrinsic characteristics for product biosynthesis (Koller et al., 2007; Xin et al., 2018; Zhgun, 2023). *C. necator* is particularly efficient for PHA production, which makes it a natural candidate for industrial-scale PHA manufacturing. However, as a wild-type strain, *C. necator* is constrained by evolutionary limitations and regulatory networks that, while allowing for general nutrient utilization, do not fully unlock its potential for efficient PHA production in the manually controlled fermentation conditions. These regulatory constraints must be overcome to maximize its performance in large-scale production, where strain robustness, process efficiency, and compatibility with industrial fermentation systems need to be optimized to achieve scalable and economically viable PHA production.

This study aims to enhance PHA industrial production by engineering *C. necator* H16B, a *C. necator* H16 derivative strain synthesizing poly (3-hydroxybutyrate-co-3-hydroxyhexanoate) (PHBH) (Yin et al., 2023). We optimized the strain for utilization of palm oil and other oil-based carbon sources, converting them into high yields of biomass and PHA. Bridging the gap between laboratory innovation and industrial application, this research addresses the critical challenge of substrate utilization efficiency in naturally occurring wild-type strains and advances sustainable and cost-effective solutions for industrial-scale PHA production. The novelty lies in combining metabolic engineering for strain optimization with hypothesis-driven troubleshooting for scale-up, achieving a reduction in both production costs and environmental impact at the production scale. Notably, our study achieves the highest PHA yield reported to date using food-grade palm oil as carbon source, reaching 264 g/L with a 100 % conversion rate in industrial-scale 150 m^3 fed-batch fermentation, setting a new benchmark in the field. This advancement highlights the scalability of our approach, showcasing the industrial feasibility of high-efficiency PHA production from oil-based feedstocks. With these achievements, our study provides a sustainable, cost-effective pathway for biopolymer production, contributing to the global shift towards a circular bioeconomy and advancing the use of oil-based substrates in large-scale industrial processes.

2. Methods

2.1. Strain and culture media

The bacteria used in this study were *C. necator* H16G (an H16 mutant able to grow in glucose and produce PHB) (Orita et al., 2012), H16B (an H16G mutant expressing a heterologous (R)-specific enoyl-CoA hydratase PhaJ, which produces PHBH with approximately 5 % 3-hydroxyhexanoate content) (Yin et al., 2023) and mutants derived from H16B. The rich medium used for growth of *C. necator* H16 was TYGA media (10 g/L tryptone, 5 g/L yeast extract, 3 g/L glucose and 3 g/L ammonium sulfate) and TYOA media (10 g/L tryptone, 5 g/L yeast extract, 1.5 g/L palm oil (or 3 g/L glucose) and 3 g/L ammonium sulfate). The concentrations of salts in the *C. necator* H16 minimal medium have been reported previously (Tang et al., 2020). Chemicals were purchased from Sinopharm Chemical Reagent Co., Ltd. (Shanghai, China) unless noted otherwise. *C. necator* H16B strains were consistently grown aerobically at 30 °C.

2.2. Fermentation conditions

C. necator H16B strains were cultured from a single colony in TYGA media for 12 h as a primary seed culture. These cultures were inoculated at 1 % into TYOA media for 14 h as second seed culture. Subsequently, these precultures were used to inoculate at 10 % (v/v) into the bioreactor with minimum media supplemented with 2.5 g/L yeast extract, 4 g/L ammonium chloride as nitrogen source and palm oil (food-grade refined palm oil from COFCO) or waste cooking oil (unpurified, obtained from Shanghai Laogang via three-phase separation from wastewater) as = carbon sources. The temperature of bioreactors was kept constant at 30 °C. The pH of each culture was maintained at 6.8 through controlled addition of 28 % ammonium solution. Stirring was controlled at speeds of 300 to 1500 rpm. The dissolved oxygen concentration was maintained above 20 % by adjusting aeration using compressed air.

Foaming, a common issue when using palm oil as substrate, was controlled through substrate-limited feeding. We observed that foam generation was closely correlated with fatty acid accumulation, particularly palmitic acid. A practical 2-min monitoring method was developed by n-hexane extraction of the fermentation broth followed by centrifugation: palmitic acid—being insoluble in both water and n-hexane and having intermediate density—accumulates between the two phases. This visual cue enabled rapid estimation of residual fatty acids and allowed timely adjustment of oil feed rate to minimize foam formation and ensure stable fermentation performance.

2.3. Plasmid and strain construction

In this study, general genetic manipulations were performed according to the standard procedures. DNA was routinely amplified by using PrimerSTAR Max DNA polymerase (Takara, China) and digested using restriction enzymes from New England BioLabs, USA. Gibson assembly (Gibson et al., 2009) was used for plasmid constructions.

Plasmids were transformed into *C. necator* H16 strains via trans-conjugation with *E. coli* S17-1. Markerless gene deletions and insertions in the *C. necator* genome were achieved following the protocol described by Insomphun et al. (2014). The strains and plasmids used in this study are described in Table 1. The sequences of oligonucleotide primers used in this study are provided in Table S1 in the supplemental material.

2.4. Transposon library sequencing

The transposon library was constructed by introducing the transposon plasmid (pUTmini-Tn5) into *E. coli* S17-1 and subsequently conjugating it with *C. necator* H16B. During conjugation, the transposase randomly inserted the transposon into the H16B genome and generating approximately 500,000 clones, providing 75-fold coverage per gene. The transposon library was collected in 50 % glycerol at a 1:1 ratio and stored at −80 °C. For the preparation of the input transposon library, the frozen library was inoculated into 100 mL of TYGA medium at an initial OD of 0.05 and cultured overnight at 220 rpm. The overnight culture was used as the seed and inoculated at 2 % (v/v) in minimal media supplemented with palm oil as carbon source in 500-mL bioreactor. Fed-batch fermentation was conducted for 24 h, and the culture was then passaged into fresh fermentation medium at an initial OD of 0.1–0.14. This process was repeated every 24 h for three days, and samples were collected at the end of each day to preserve the transposon libraries. The preserved libraries were sent to Novogene Co., Ltd. (Beijing, China) for sequencing library preparation and sequencing analysis.

To analyze the Tn-Seq sequencing data and identify key genes essential for growth, the raw sequencing data was processed through quality control and alignment steps. Cutadapt (v4.4) (Martin, 2011) was used to select reads containing the transposon insertion tag sequence (CACTTGTGTATAAGAGTCAG), with parameters set to -O 17 (minimum match length) and -e 0.2 (maximum allowable error rate). Reads that did not match the tag sequence were discarded to ensure high-quality data. The filtered reads were aligned to the *C. necator* H16 reference genome (GCA_000009285.2) using the tpp.py script from TRANSIT (v3.3.1) (DeJesus et al., 2015), with BWA (v0.7.17) (Li and Durbin, 2009) and the MEM algorithm. The transposon insertion tag sequence (TTGTGTATAAGAGTCAG) was specified as a primer during alignment. The alignment data were normalized using the Trimmed Total Reads (TTR) method to correct for differences in sequencing depth and batch effects across samples. Normalized data were further analyzed using the resampling method in TRANSIT's transit.py script. Differential analyses were conducted by comparing samples from day 0 (input library) with those from day 1, day 2, and day 3. This approach enabled the identification of conditionally essential genes under the tested growth conditions.

Table 1
Strains and plasmids used in this study.

Strains or plasmids	Description	Source or reference
Cupriavidus necator		
H16G	Parental strain	Orita et al. (2012)
H16B	H16G derivative; (*R*)-specific enoyl-CoA hydratase *PhaJ*	Yin et al. (2023)
Δ*mutS*	H16B derivative; ΔmutS	This study
ΔA3043	H16B derivative; ΔA3043	This study
ΔA3044	H16B derivative; ΔA3044	This study
ΔA3043/ ΔA3044	H16B derivative; ΔA3043/ΔA3044	This study
ΔA3043/lipAB	ΔA3043 derivative; *H16_A1322* and *H16_A1323*	This study
Escherichia coli		
DH5α	General cloning strain	Invitrogen, USA
S17-1	Strain for conjugative transfer of plasmids to *C. necator*	Simon et al., 1983
Plasmids		
pK18mob	The backbone used to make other plasmids for gene deletion/insertion in *C. necator* genome	Orita et al. (2012)
pKO-ΔmutS	Plasmid for deletion of *mutS* from *C. necator* genome	This study
pKO-ΔA3043	Plasmid for deletion of *H16_A3043* from *C. necator* genome	This study
pKO-ΔA3044	Plasmid for deletion of *H16_A3044* from *C. necator* genome	This study
pKO-ΔA3043+ A3044	Plasmid for deletion of *H16_A3043* and *H16_A3044* from *C. necator* genome	This study
pKI-lipAB	Plasmid for insertion of *H16_A1322* and *H16_A1323* into *C. necator* genome	This study
pUTmini-Tn5	Plasmid for transposon library construction	This study

2.5. Adaptive evolution

The Δ*mutS* strain was grown on TYGA agar plates, from which two independent single colonies were inoculated into TYGA broth and cultured for 16 h. These cultures were then diluted at a 25 % (v/v) ratio into TYOA medium and cultured for 4 h as starting cultures. For adaptive evolution, the starting cultures were inoculated into 500-mL bioreactors with 1.5 g/L palm oil at a 2 % (v/v) ratio and subjected to serial passaging every 12 h for 25 passages across two independent lineages. Each passage was inoculated to achieve a final OD of 0.1, and cultures were preserved at every step. To assess evolutionary outcomes, preserved cultures from the final passage and starting culture were streaked on plates to isolate single clones. These clones were grown in 24-deep well plates using TYGA medium for 16 h and then transferred to fresh fermentation medium at an initial OD of 0.05. OD measurements were taken every 2 h by a custom-designed high-throughput, flexible automation platform to generate growth curves, identifying clones with growth advantages over the starting clones. Clones showing growth advantages over the starting clones were subjected to genome sequencing analysis for further investigation of adaptive mutations.

To analyze the mutations of clones with growth advantages, Illumina NovaSeq 6000 platform was used for 150 bp paired-end sequencing. Raw sequencing data was subjected to quality control using fastp (v0.23.2) (Chen et al., 2018) with default parameters, filtering out low-quality reads, removing adapter sequences, and deleting reads shorter than the minimum length to generate high-quality clean data. The cleaned reads were then aligned to the *C. necator* H16 reference genome (GCA_000009285.2) using the BWA tool (v0.7.17) (Li and Durbin, 2009) with the MEM algorithm. The alignment results were processed using Picard (v2.27.4) ("Picard Tools - By Broad Institute," 2024), where the MarkDuplicates module was used to mark PCR duplicates and reduce the impact of duplicate sequences on variant detection. SNP variants were called using GATK (v4.4.0.0) (Cibulskis et al., 2013) with the Mutect2 module, enabling mitochondrial mode (–mitochondria-mode true) for accurate variant calling. Preliminary variant filtering was performed using the FilterMutectCalls module of GATK, with parameters set to –max-alt-allele-count 100 and –unique--alt-read-count 5 to ensure the reliability of the identified variants. Finally, all variants were functionally annotated using snpEFF (v5.1c) (Cingolani et al., 2012), which provided insights into the functional impact of each SNP, such as missense mutations, synonymous mutations, and other functional annotations.

2.6. PHA assays via gas chromatography (GC)

The bacterial cells were harvested and centrifuged at 10,000 g for 10 min. Dry cell weight (DCW) was determined after drying. The PHA contents were then analyzed using gas chromatography (GC-2010 Pro, SHIMADZU, Japan) as previously described (Sheu and Lee, 2004).

2.7. Metabolomics analysis

C. necator H16B and ΔA3043 samples in 500-mL fed-batch fermentations were collected at 10 h and 32 h post inoculation using 2.0 mL grinding tubes (Jingxin, China). Each grinding tube was added with 405 μL of the reagent prepared by mixing MEOH and H_2O at a ratio of 5:4, two 3.2 mm grinding beads (Jingxin, China), and 750 μL methyl tert-butyl ether (MTBE). The homogenate was ground using a grinder (Jingxin, China) at 4 °C, 30 Hz, for four cycles of 15 s with a 15 s interval. The sample was then centrifuged in a centrifuge (Eppendorf, Germany) at 15,000 rpm for 10 min at 4 °C. 100 μL of the lower phase metabolite fraction was taken out, diluted with 300 μL of ACN:MEOH (1:1), and placed in a −80 °C refrigerator overnight for protein precipitation. Before injection, the sample was centrifuged at 15,000 rpm for 10 min, and then 100 μL was transferred into an injection vial for metabolomics LC-MS analysis. An equal-proportion sampling from each test sample was mixed to form a quality control (QC) for evaluating the instrument stability.

Untargeted metabolomics data acquisition was performed using a Shimadzu LC system coupled to a TripleTOF mass spectrometer (QTOF 6600+, ABSciex, made in Woodlands Central Industrial Estate, Singapore). Chromatographic separation was achieved using a HILIC column (IHILIC-(P) Classic column, 5 μm, 150 mm × 2.1 mm, 200 A, made in Sweden). The mobile phase A was 20 mmol/L ammonium acetate, 0.1 % ammonium hydroxide, and 2.5 μmol/L methylene diphosphate in 95:5 water:ACN, and mobile phase B was ACN. The gradient was as follows: 0 min, 85 % B; 2 min, 85 % B; 7 min, 65 % B; 12 min, 35 % B; 12.1 min, 20 % B; 15.9 min, 20 % B; 16 min, 85 % B; 23 min, 85 % B. The flow rate was set at 0.2 mL/min with a sample injection volume of 5 μL and the total run time at 23 min. ESI parameters setup was GS1, 60; GS2, 60; CUR, 35; temperature, 500; ISVF, −4500 in negative modes. Peak area for each metabolite was integrated using El-MAVEN software (version 0.12.1).

2.8. Transcriptomics analysis

C. necator H16B and ΔA3043 samples were collected at 10 h and 32 h of 500-mL fed-batch fermentation and total RNA was isolated from the cell pellet using Trizol reagent (Invitrogen, USA) according to the manufacturer's instructions. Following total RNA extraction, a chromosome-specific complementary DNA (cDNA) library was constructed utilizing the Illumina TruSeq Stranded RNA Library Prep Kit (Illumina, San Diego, USA). The library was sequenced on the Illumina NovaSeq 6000 platform employing 150 bp paired-end sequencing methodology, with the resultant raw data being utilized for subsequent analyses. The raw sequencing data were subjected to quality control using fastp (v0.23.2) (Chen et al., 2018) with default parameters to filter out low-quality reads, eliminate adapter sequences, and discard reads of insufficient length, thereby generating high-quality clean data. The filtered reads were aligned to the *Cupriavidus necator H16* reference genome (GCA_000009285.2), and transcript-level expression values were computed using salmon (v1.10.1) (Patro et al., 2017). Standardized expression values including Transcripts Per Million (TPM) and Counts were generated. Differential expression analysis was conducted utilizing the DESeq2 (v1.38.3) (Love et al., 2014) R package, applying a screening criterion of p-value <0.01 and $|\text{Fold Change}| > 2$; differentially expressed genes identified through this process were subsequently analyzed further. Functional enrichment analysis of differentially expressed genes was performed using the R package clusterProfiler (v4.8.1) (Wu et al., 2021), based on pathway enrichment assessments from the KEGG database, with statistical significance set at p-value <0.05.

2.9. Stress response to phosphorus limitation

To investigate the metabolic stress response, *C. necator* H16B and ΔA3043 strains, were first grown in TYGA media for 12 h. After incubation, the cultures were centrifuged, and the cell pellets were washed twice with Salt Solution (a nitrogen- and phosphorus-free minimum salt medium, remove NH_4Cl, Na_2HPO_4, KH_2PO_4 from the minimum media, and replace Fe(III)-NH_4-Citrate in the minimum media with Fe(II)SO4 and Citrate) to remove excess nutrients. The washed cells were then resuspended in the phosphorus-free medium (Salt Solution + 10 g/L palm oil, 0.9 g/L polyglycerol ester of oleic acid, 1 g/L NH_4Cl, and 40 mM MOPS (3-(N-morpholino)propanesulfonic acid)). These resuspended cultures were inoculated into 24-deep well plates at 220 rpm for 0, 2, 12, 24, 48, and 72 h. At each time point, dilutions of cultures were plated on agar plates, and colony-forming units (CFU) were counted to assess the growth response of the strains under phosphorus limitation.

2.10. Thin layer chromatography (TLC) analysis

One mL of *C. necator* H16B and ΔA3043 samples in 200-L fed-batch cultures were collected at different time points and mixed with 200 μL n-hexane. After vortexed for 5 s, the mixtures were centrifuged at 12,000 g for 2 min, and the lipid extracts in the organic phase were separated on Silica gel F254 (0.25 mm or 0.5 mm, MERCK, Germany) and developed with a solvent system consisting of n-hexane: ethyl acetate: acetic acid (10:1:1, v:v:v). After drying, the TLC plates were visualized by either ultraviolet light ($\lambda = 254$ nm) or colorimetric sulfo-phospho-vanillin (SPV) method (Johnson et al., 1977).

2.11. Lipase activity assay

C. necator H16B strains (ΔA3043 and ΔA3043/lipAB) were cultured from a single colony in TYGA medium for 12 h as a primary seed culture. These cultures were then inoculated at 1 % (v/v) into TYOA medium and grown for 6 h. The fermentation broth was subsequently centrifuged, and the uppermost grease layer was carefully removed using a sterile cotton swab. The resulting supernatant was transferred into a 1.5 mL centrifuge tube. Lipase activity was measured using the Lipase Activity Assay Kit (BC2340; Beijing Solarbio Science & Technology, Beijing, China) according to the manufacturer's instructions.

2.12. Carbon footprint analysis

The process was modeled using palm oil and waste cooking oil, with *C. necator* H16B and ΔA3043/lipAB applied at 150 m^3 fed-batch fermentation. The life cycle assessment was based on the average outcome of PHA production. The material input and output under different scenarios are listed in Tables S2 and S3. Inventory data for materials and utilities were based on the PHA production plant of Bluepha located in Yancheng, China, without any data selection or modification. The life cycle assessment (LCA) was conducted in accordance with ISO 14044/40 guidelines ("ISO 14040," 2025). The assessment followed a cradle-to-gate boundary, encompassing upstream emissions from raw materials, utility consumption, waste air emissions and wastewater effluents, and transportation. Both ReCiPe midpoint and endpoint (H) calculations were applied. Carbon intensities for each variable were sourced from the Ecoinvent 3.9 database (Wernet et al., 2016).

All material and utility data (Tables S2 and S3) are based on CN-type data. If specific CN data is unavailable, RoW (Rest of the World) data will be used as a substitute. Malaysia-based palm oil data was selected to accurately reflect the real purchasing scenario. For electricity consumption, data was sourced from the Eastern China scenario, using the proportional distribution of electricity sources in Yancheng City.

3. Results

3.1. Comparison of glucose and palm oil as carbon sources for PHA production using Cupriavidus necator

C. necator is capable of utilizing both glucose and palm oil as sole carbon sources for PHA production (Fig. 1A). Both glucose and palm oil are metabolized into acetyl-CoA, which is further converted into 3-hydroxybutyryl-CoA (3HB-CoA), the primary monomer for PHA synthesis. The polymerization of 3HB yields polyhydroxybutyrate (PHB), a homopolymer type of PHA. Additionally, palm oil undergoes fatty acid oxidation (FAO) to generate acyl-CoA, which is then converted by the enoyl-CoA hydratase PhaJ into 3-hydroxyacyl-CoA. This can co-polymerize with 3HB to form copolymers, such as poly (3-hydroxybutyrate-co-3-hydroxyhexanoate) (PHBH) (Fig. 1A), which has different properties compared to PHB. PHBH exhibits decreased crystallinity and improved mechanical performance, due to its combination of crystalline (3HB) and elastomeric (3-hydroxyhexanoate, 3HHx) units. We confirmed that using palm oil as the sole carbon source, *C. necator* H16G produced PHB, while *C. necator* H16B, a mutant strain of H16G expressing a heterologous (R)-specific enoyl-CoA hydratase PhaJ (Yin et al., 2023), produced approximately 5 % PHBH in the 500-mL fed-batch fermentation (Fig. 1B and C). These results demonstrate that palm oil is a suitable carbon source for producing a wider variety of PHA types using different *C. necator* strains.

We evaluated the theoretical substrate cost for PHA production. To simplify the calculation, PHB was used as a representative PHA, and palmitate was used to representpalm oil. One molecule of glucose (6 carbons) is converted into 2 acetyl-CoA molecules ($2 \times 2 = 4$ carbons) through the Entner–Doudoroff (ED) glycolysis pathway for PHA production, while one molecule of palmitate (16 carbons) is converted into 8 acetyl-CoA molecules ($2 \times 8 = 16$ carbons) via FAO (Fig. 1D). Therefore, the theoretical molar carbon conversion rate for glucose is 66.7 % and that for palmitate is 100 % (Fig. 1E). The typical commodity prices for sugar and palmitate are around $470 and $950 per ton, respectively. As a result, the theoretical substrate cost per ton of PHB is $825 using sugar, compared to $590 using palmitate, indicating that palm oil is a more economical carbon source for PHA production (Fig. 1E).

To assess actual productivity, fed-batch fermentations of *C. necator* H16B were conducted in 2-L bench-scale bioreactors with glucose and palm oil as sole carbon sources (Fig. 1F). The results showed that, compared to using glucose, using palm oil led to significantly higher biomass accumulation and PHA yields, with significantly lower substrate consumption in weight, (Fig. 1F and G). The mass conversion rate (g PHA yield/g substrate consumed) of glucose was only 34 %, corresponding to a $1382 substrate cost per ton of PHB, whereas palm oil achieved a conversion rate of 87 %, corresponding to a $1092 substrate cost. Together, these results demonstrate that palm is a superior carbon source for PHA production, offering higher yields, lower cost, and the ability to produce a variety of PHA types.

3.2. Screening and identification of mutants with enhanced oil consumption and PHA production

Substrate utilization efficiency is a key factor affecting the PHA productivity and, consequently, production cost. As *C. necator* H16B has not been optimized for consuming oil for PHA production, we sought to identify mutants with enhanced oil consumption and unimpaired PHA production. We hypothesized that enhanced oil consumption could confer a selective growth advantage, and therefore, used two orthogonal approaches, transposon sequencing (Tn-seq) and adaptive evolution, to screen for mutants with increased palm oil consumption (Fig. 2A). In the Tn-seq approach, a transposon mutant library was passaged in two independent lineages for 4 days with palm oil as the sole carbon source in 500-mL bioreactors (in order to represent the fermentation condition). Mutants that exhibited significant enrichment during cultivation were identified (Table S4). Among them, *H16_A3043* and *H16_A3044* mutants showed significant enrichment in both lineages (Fig. 2B–S1), and the enrichment continued to increase over time (Fig. 2C–S1). In the adaptive evolution approach, we generated a hypermutation strain by knocking out the *mutS* genes (Siegel and Bryson, 1967), speeding up the evolution with a 100-fold increase in the spontaneous mutation rate compared to the wild-type strain (Fig. S2). The Δ*mutS* strain was cultured with palm oil as the sole carbon source in two independent lineages for 25 passages in 500-mL bioreactors. The growth curves of single isolates using palm oil were monitored in 24-well plates using a custom-designed high-throughput, flexible automation platform (Fig. 2D–S3A). The isolates exhibiting growth advantages were genome sequenced to identify mutations (Fig. S3B). We found that severe mutations, such as frameshift mutations in *H16_A3043*, were frequently associated with mutants exhibiting a growth advantage, while isolates with no mutation or non-coding mutation did not show a growth advantage (Fig. 2E and F, S3B, S3C).

H16_A3044 is annotated as a histidine kinase, and *H16_A3043* is annotated as a NarL family transcription factor. Similar fitness patterns between these two neighboring genes suggest they likely form a two-component signal sensing and transduction system (TCS). The annotations of these two genes and those genes in the immediate genomic neighborhood do not suggest any information about the external stimulus that the system responds to, or the genes whose expression the system might be regulating. To confirm their roles in palm oil consumption, we generated knockout strains for each gene, as well as a double knockout strain, and tested their performance in the 500-mL fed-batch fermentation using palm oil as feedstock. The results showed that the knockout of either or both genes led to significantly increased oil consumption, higher PHA yield, and improved conversion efficiency compared to H16B (Fig. 2G and H). We also created mutants of other loci identified from Tn-seq and adapted evolution experiments, but no mutant exhibited as dramatic growth advantage compared to H16B (Fig. S4). These findings suggest *H16_A3043* and *H16_A3044* as an effective gene target for enhancing palm oil consumption and PHA biosynthesis in *C. necator*.

3.3. H16_A3043/H16_A3044 is a global regulator of biogenesis and stress response

To further elucidate the role of *H16_A3043/H16_A3044* in oil consumption and PHA production, we conducted detailed metabolomic and transcriptomic analyses. Since knocking out either or both genes resulted in similar growth rates, oil consumption and PHA production (Fig. 2G and H), the transcriptional regulator ΔA3043, the knockout of which fully abolishes the regulatory function of the two-component system, was selected for further mechanistic studies. Samples were collected during 500-mL fed-batch fermentation at two key time points: the logarithmic growth phase (10 h), characterized by rapid cell division, and the PHA synthesis phase (32 h), marked by rapid PHA accumulation (Fig. S5).

Metabolomic profiling revealed global changes at both time points, with more pronounced alterations observed at 32 h (Fig. 3A, S6A). In ΔA3043, acetyl-CoA levels were significantly elevated, while palmityl-CoA and stearoyl-CoA levels were reduced, indicating enhanced β-oxidation. This upregulation provides more acetyl-CoA for energy production and PHA biosynthesis. Additionally, 3HHx and 3HB, likely derived from 3HHx-CoA and 3HB-CoA degradation, were markedly reduced, particularly at 10 h, consistent with increased PHA biosynthesis by channeling 3HHx-CoA and 3HB-CoA to PHA biosynthesis rather than degradation. This observation aligns with the increased cellular PHA content in ΔA3043 at both 10 h and 32 h (Fig. 3B).

In addition to fatty acid metabolism, nucleotide biosynthesis pathways were consistently upregulated in ΔA3043 compared to H16B at both time points (Fig. 3A–S6A), correlated with faster cell growth

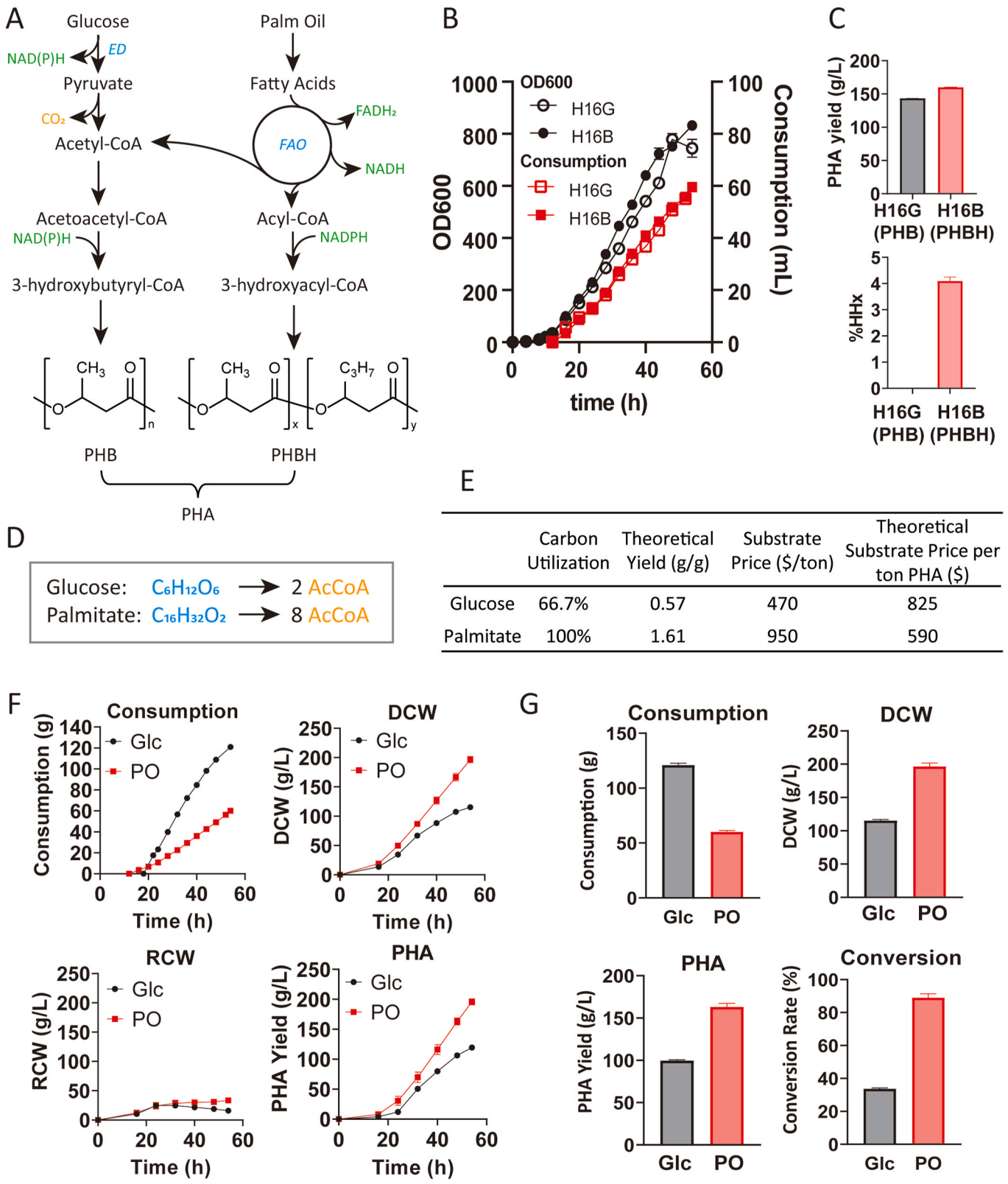

	Carbon Utilization	Theoretical Yield (g/g)	Substrate Price ($/ton)	Theoretical Substrate Price per ton PHA ($)
Glucose	66.7%	0.57	470	825
Palmitate	100%	1.61	950	590

Fig. 1. Comparison of using sugar and palm oil as sole carbon sources for PHA production in *C. necator*. **(A)** Schematic biosynthetic pathways for PHA production using glucose and palm oil as carbon sources in *C. necator* H16B. **(B–C)** PHB and PHBH production by *C. necator* H16G and H16B, respectively, using palm oil as the substrate in a 500-mL fed-batch fermentation. **(D)** Theoretical stoichiometry comparison between glucose and palmitate as carbon sources for PHA production. **(E)** Cost comparison between glucose and palm oil as carbon sources based on the average commodity prices for sugar and palm oil from May to November 2024. **(F–G)** Substrate consumption, dry cell weight (DCW), residual cell weight (RCW), PHA yield, and conversion rates in the 2-L fed-batch fermentation using glucose (Glc) and palm oil (PO) as substrates. Data are shown as means ± SEM, n ≥ 3.

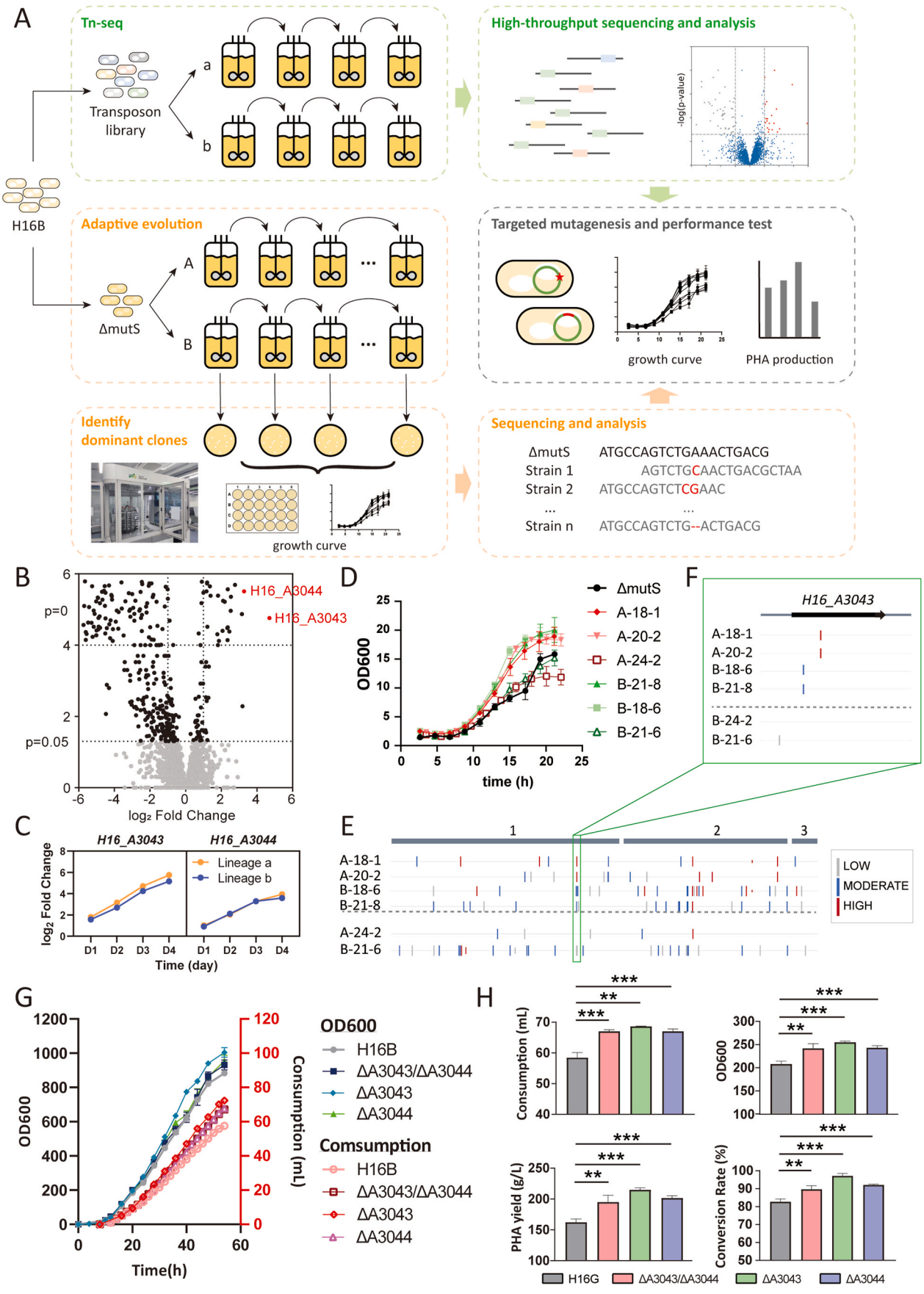

(caption on next page)

Fig. 2. Screening for high-oil consumption strains. **(A)** Schematic representation of the dual screening strategy, combining transposon sequencing (Tn-seq) and adaptive evolution approaches, used to identify mutants with enhanced palm oil utilization. **(B)** Representative volcano plot of the Tn-seq analysis showing frequency changes of transposon insertion mutants from lineage A after 4 days of growth using palm oil as the sole carbon source. **(C)** Log2 fold change of *H16_A3043* and *H16_A3044* mutant frequencies over time in both lineages of the Tn-seq screen. **(D)** Growth curves of selected strains isolated during 25 passages of adaptive evolution. Solid red: isolates with growth advantage in lineage A; Hollow red: isolates without growth advantage in lineage A; Solid green: isolates with growth advantage in lineage B; Hollow green: isolates without a growth advantage in lineage B; Black: Δ*mutS* control strain. **(E)** Mutation profile of the selected strains in (D). Red: frameshift or premature stop codon mutations; Blue: amino acid substitutions; Gray: synonymous mutations or non-coding sequence mutations. Mutants above the dashed line showed a growth advantage, while those below did not. **(F)** Zoomed-in view of the mutation in the *H16_A3043* gene. **(G)** Growth curves and palm oil consumption rates of *H16_A3043* and/or *H16_A3044* knockout mutants (ΔA3043 and/or ΔA3044). **(H)** Comparison of palm oil consumption, OD600, PHA yield, and conversion rate between the knockout strains, demonstrating improved performance in all metrics. Data are shown as means ± SEM, n ≥ 3. Statistical significance was determined using a two-tailed Student's t-test (**p < 0.01, ***p < 0.001). (For interpretation of the references to color in this figure legend, the reader is referred to the Web version of this article.)

(Fig. 2G). During the PHA synthesis phase, nucleotide biosynthesis intermediates in H16B significantly decreased, with metabolites such as AICAR and FGAR falling below detectable levels (Fig. 3C–S6B). By contrast, these intermediates in ΔA3043 showed less reduction and maintained higher levels compared to H16B, indicating that ΔA3043 continued attempting to divide despite environmental changes.

We hypothesize that the *H16_A3043/H16_A3044* two-component system plays a role in regulating cell growth upon stress. To test this hypothesis, ΔA3043 and H16B were cultured in phosphorus-free media as an example of environmental stress. In nutrient-rich media, ΔA3043 exhibited a faster division rate without a lag phase compared to H16B. However, in phosphorus-free media, ΔA3043 displayed a much faster decline in viable cell numbers over time (Fig. 3D). After 72 h, the survival rate of ΔA3043 was approximately 5 % that of H16B. This compromised stress adaptation could be explained by that ΔA3043 continued cellular division regardless of nutrient limitation.

RNA-seq analysis confirmed the impaired stress response and increased cellular metabolic activity in ΔA3043 (Fig. 3E). Genes associated with chemotaxis, motility, and environmental response, including bacterial-type flagellum assembly, chemotaxis, and signal transduction, were consistently downregulated. Conversely, pathways related to cellular biogenesis and metabolic activities, such as type IV pilus assembly, biotin biosynthesis, and ubiquinone biosynthesis, were upregulated, particularly at 32 h. Notably, genes involved in flagellum formation, critical for swimming motility, were downregulated, while type IV pilus genes, associated with swarming motility, were upregulated, indicating impaired cellular motility. This trade-off between metabolic enhancement and motility suppression is consistent with previous observations, where *C. necator* reduces flagellation during PHA synthesis (Raberg et al., 2008), and PHB accumulation inhibits chemotaxis and motility gene expression in *Bradyrhizobium diazoefficiens* (Quelas et al., 2024). Overall, the enhanced PHA production in ΔA3043 is accompanied by dysregulation of motility and chemotaxis pathways, reflecting a trade-off that reduces stress adaptation in natural environments. However, this limitation is mitigated in manually controlled, nutrient-rich fermentation systems, where ΔA3043 demonstrates superior production capabilities.

3.4. Lipase engineering enhanced the scalability of fed-batch fermentation to pilot-scale

Building upon the mechanistic insights into the *H16_A3043/H16_A3044* two-component system, we next evaluated the scalability of the engineered strain for industrial application. Despite the clear metabolic advantages observed in laboratory-scale fermentations, the impaired environmental stress adaptability of ΔA3043, coupled with the strain's altered lipid metabolism, highlighted potential bottlenecks that could impact scalability. In the 200-L fed-batch fermentation system, compared to H16B, ΔA3043 exhibited a higher oil consumption rate, higher biomass and PHA yields, demonstrating a potential productivity advantage (Fig. 4A). However, we observed large amounts of sludge formed at 20–30 h during fermentation. This sludge was clearly visible through the fermentation tank window and also precipitated at the fermentation ports and pipes (Fig. 4B), significantly impairing the fermentation process and downstream processing. The sludge appeared as a cluster of oil and bacterial cell aggregates under the microscope. To investigate this phenomenon, we used Thin Layer Chromatography (TLC) to monitor and compare the oil and fatty acid content in the fermentation samples at different time points during the 500-mL and 200-L fed-batch fermentations. The results showed that both oil and fatty acid contents decreased over time in 500-mL fermentation, while they increased from 20 h in the 200-L fermentation (Fig. 4C), indicating impaired oil consumption capacity at the larger scale, which likely correlated with the formation of sludge.

While β-oxidation was enhanced in ΔA3043, the reduced level of palmityl-CoA and stearoyl-CoA (Fig. 3A–S6A) indicated insufficient carbon source supply inside the cell. The depletion of palmityl-CoA and stearoyl-CoA suggests that while β-oxidation is enhanced, the availability of fatty acid-derived intermediates is insufficient to sustain metabolic demands. To determine whether fatty acid transport or lipid hydrolysis is the limiting factor, we constructed a strain (ΔA3043/FadL) in which the fatty acid transport protein FadL from *Ralstonia pickettii* (NCBI Reference Sequence: WP_012430599.1) was heterologously expressed. However, the oil consumption rate, growth rate, and PHA production of ΔA3043/FadL were nearly identical to those of ΔA3043, indicating that fatty acid uptake is not the bottleneck (Fig. S7). We reasoned that there was an imbalance between fatty acid supply into the cell and fatty acid utilization within the cell. Compared to sugars, lipids must first be hydrolyzed by extracellular lipase into fatty acids (and glycerol) before being transported and utilized by bacterial cells (Rao et al., 2010). The availability of the oil substrate to the bacterial cells is thus dependent on the lipase activity (Kumar et al., 2020). Indeed, the transcriptional level of lipase genes *lipAB* (*H16_A1322-H16_A1323) was not elevated in* ΔA3043 *(*Table S6*)*, despite the enhanced oil consumption. To further investigate the role of lipase expression in oil metabolism, we constructed a lipase promoter disruption strain. In 500-mL fed-batch fermentation, this mutant exhibited severely impaired growth, with an OD of only 3.8 after 8 h, while dissolved oxygen remained above 95 %, indicating minimal metabolic activity. In contrast, ΔA3043/lipAB achieved an OD of over 20 at the same time point, demonstrating significantly improved growth and oil utilization. These results confirm that lipase expression is essential for palm oil metabolism, and its disruption severely impairs fermentation performance, further supporting the need for enhanced lipase expression. We hypothesized that due to insufficient lipase expression, the unutilized oil caused the bacterial cell aggregates and hindered the bacteria to efficiently utilize substrate from the fermentation. To test this hypothesis, we introduced a medium-strength constitutive promoter upstream of the coding region of the *lipAB* genes in ΔA3043 and constructed a lipase overexpression strain, ΔA3043/lipAB. This strain achieved an 11-fold stable increase in lipase expression and 3-fold increase in lipase activity (Fig. S8), effectively enhancing triglyceride hydrolysis, particularly in the vicinity of bacterial cells. The TLC results of the ΔA3043/lipAB 200-L fermentation showed that no oil or fatty acid accumulated during the fermentation process (Fig. 4D). This modification successfully resolved the sludge formation issue and further enhanced biomass, PHA

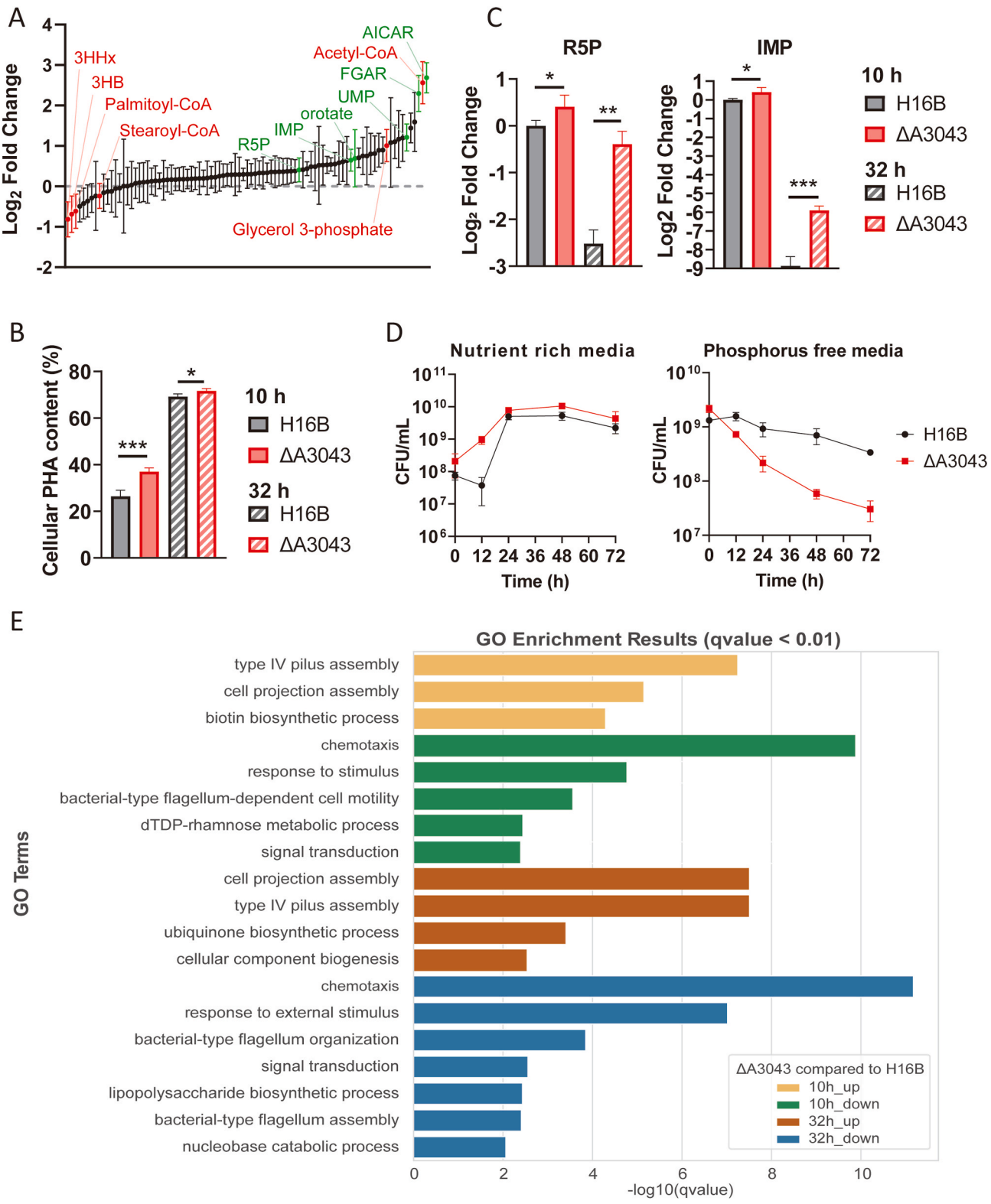

Fig. 3. Mechanism of the *H16_A3043/H16_A3044* two-component system in enhancing oil consumption and PHA production. **(A)** Log2 fold change of metabolites in ΔA3043 compared to H16B at 10 h, normalized to residual cell mass. Metabolites associated with fatty acid oxidation and PHA biosynthesis are labeled in red, while those involved in nucleotide biosynthesis are labeled in green. **(B)** Percentage of PHA in biomass in ΔA3043 compared to H16B at 10 h and 32 h. **(C)** Log2 fold change of ribose-5-phosphate (R5P) and inosine monophosphate (IMP) in ΔA3043 compared to H16B at 10 h and 32 h, normalized to residual cell mass. **(D)** Growth curves of ΔA3043 and H16B in nutrient-rich and phosphorus-free media. **(E)** Gene transcription enrichment analysis in ΔA3043 compared to H16B at 10 h and 32 h. Data are shown as means ± SEM, n ≥ 3. Statistical significance in (B) and (C) was determined using a two-tailed Student's t-test (*p < 0.05, **p < 0.01, ***p < 0.001). (For interpretation of the references to color in this figure legend, the reader is referred to the Web version of this article.)

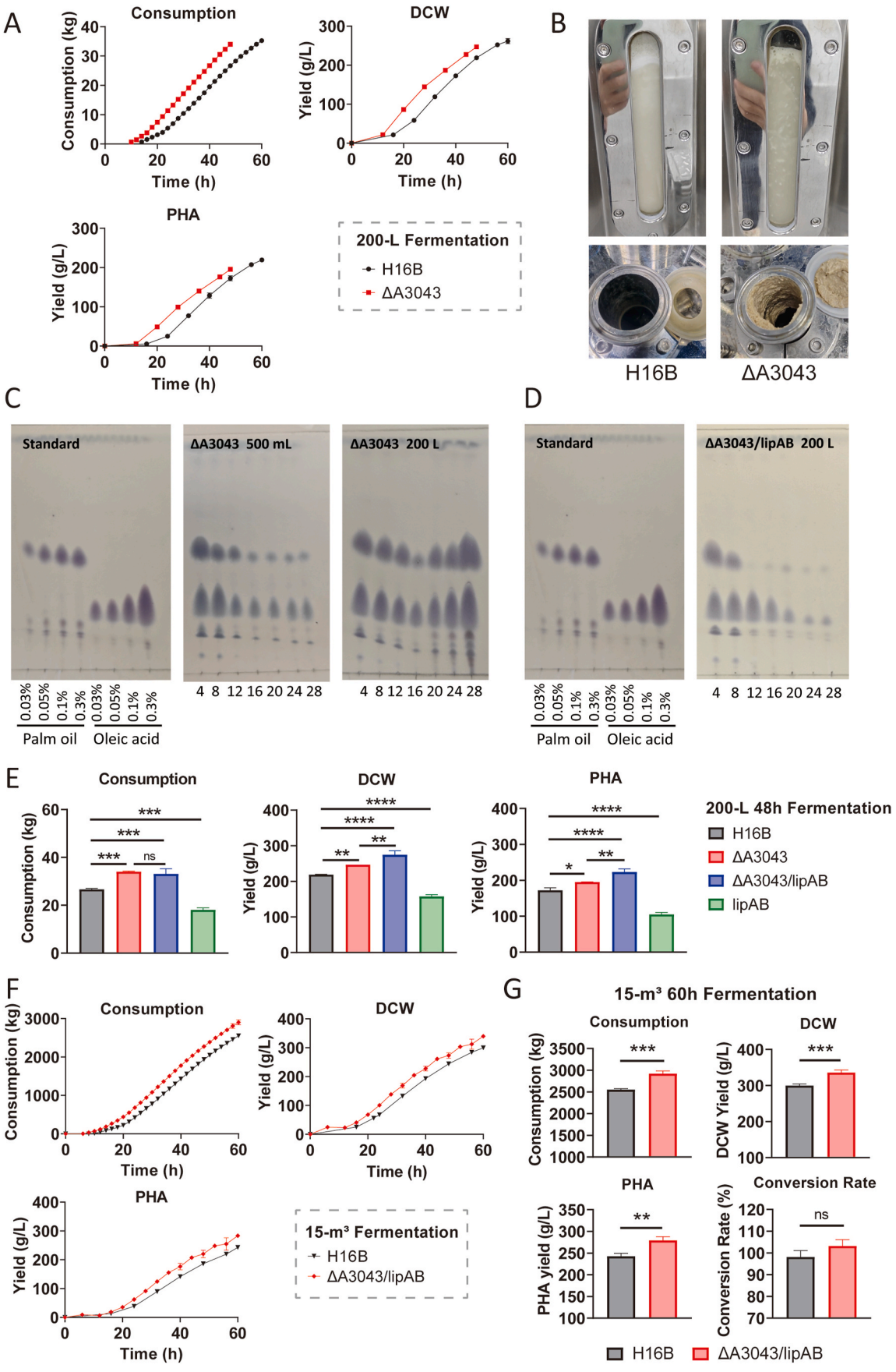

(caption on next page)

Fig. 4. Performance and troubleshooting of H16B engineered mutants in large-scale fed-batch fermentation. **(A)** Palm oil consumption, biomass, and PHA yield in the 200-L fed-batch fermentation of ***C. necator* H16B** and **ΔA3043. (B)** Photographs of the fermenter window and feeding port taken during the fermentation of **H16B** and **ΔA3043**. **(C)** Thin layer chromatography (TLC) results showing the residual amount of palm oil and fatty acid in **ΔA3043** samples at different time points during the 500-mL and 200-L fed-batch fermentation. **(D)** TLC analysis of **ΔA3043/lipAB** samples at different time points during the 200-L fed-batch fermentation. **(E)** Comparison of palm oil consumption, biomass, and PHA yield between H16B, **ΔA3043, ΔA3043/lipAB, and lipAB at 48 h in 200-L fed-batch fermentation.** Data are shown as means ± SEM, n ≥ 2. Statistical significance was determined using one-way ANOVA with Tukey's multiple comparisons test (ns not significant, *p < 0.05, **p < 0.01, ***p < 0.001, ****p < 0.0001). **(F–G)** Comparison of palm oil consumption, biomass, PHA yield, and conversion rates between **ΔA3043/lipAB** and **H16B** in the 15-m^3 fed-batch fermentation, showing improved performance for **ΔA3043/lipAB** across all metrics. Data are shown as means ± SEM, n ≥ 2. Statistical significance was determined using a two-tailed Student's t-test (ns not significant, **p < 0.01, ***p < 0.001).

yield, oil consumption rate compared to H16B at the 200-L scale (Fig. 4E). The lipase overexpression alone did not confer enhanced oil consumption, as the strain overexpressing *lipAB* without deleting *H16_A3043* exhibited disadvantages compared to H16B in the fed-batch fermentation (Fig. 4E). Building upon the 200-L success, further scale-up of ΔA3043/lipAB to the 15-m^3 pilot-scale showed a 15.0 % increase in PHA yield, a 14.4 % increase in oil consumption, and a 5.1 % improvement in the conversion rate in the 60-h fed-batch fermentation (Fig. 4F and G). Together, these results validated lipase engineering as a hypothesis-driven troubleshooting solution to the industrialization scale-up challenge of the ΔA3043 strain in PHA production.

3.5. *Scale-up of ΔA3043/lipAB fermentation and evaluation of waste cooking oil as an alternative feedstock for PHA production*

To achieve our production goals, we further scaled up ΔA3043/lipAB

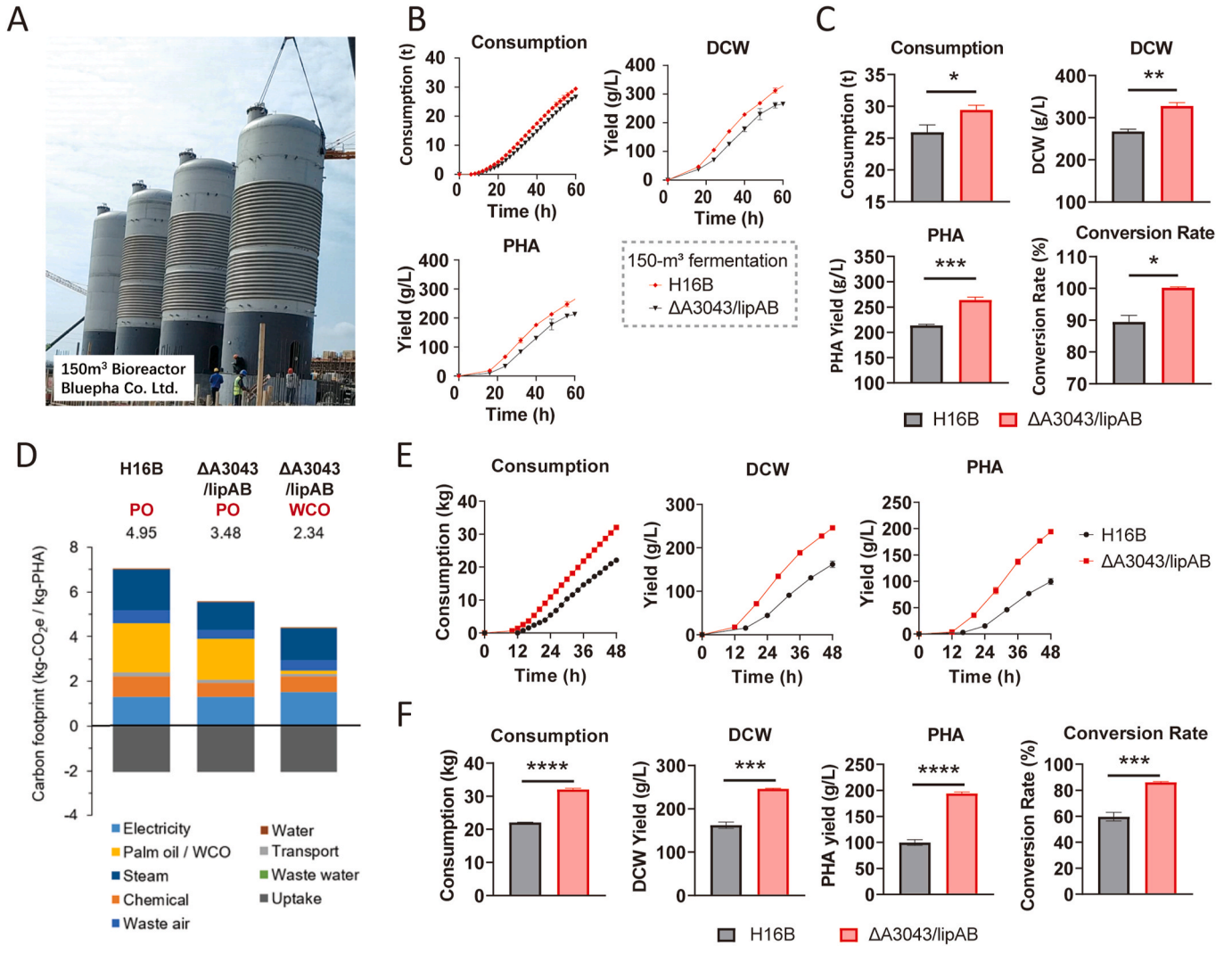

Fig. 5. Performance of ΔA3043/lipAB in large-scale fermentation with palm oil and waste cooking oil as carbon sources. **(A)** Photographs of the production-level 150-m^3 fermenter used for PHA production. **(B)** Palm oil consumption, biomass, and PHA yield of H16B and ΔA3043/lipAB using palm oil feedstock in the 150-m^3 fed-batch fermentation. **(C)** Comparison of end-point metrics between H16B and ΔA3043/lipAB using palm oil in 150-m^3 fermentation, demonstrating the superior performance of ΔA3043/lipAB. **(D)** Cradle-to-grave carbon footprint comparison between H16B and ΔA3043/lipAB using different oil feedstocks, highlighting a reduced environmental impact using ΔA3043/lipAB and waste cooking oil (WCO). **(E)** Palm oil consumption, biomass and PHA yield of H16B and ΔA3043/lipAB using waste cooking oil as the carbon source in the 200-L fed-batch fermentation. **(F)** Comparison of end-point metrics between H16B and ΔA3043/lipAB using WCO, showing enhanced performance of ΔA3043/lipAB in WCO fermentation. Data are shown as means ± SEM, n ≥ 2. Statistical significance was determined using a two-tailed Student's t-test (*p < 0.05).

fed-batch fermentation to the 150 m^3 production scale. ΔA3043/lipAB demonstrated significantly improved performance compared to H16B, with higher oil consumption, biomass accumulation, PHA yield, and conversion rates. Specifically, ΔA3043/lipAB achieved a final PHA yield of 264 g/L and 3.05 tons per batch, representing a 25.4 % increase in yield and a 5.6 % improvement in conversion rate compared to H16B, with a mass conversion rate of 100 % after 60 h of fermentation (Fig. 5A and B). These results demonstrated the strain's robustness under industrial-scale processes, highlighting the feasibility of transferring laboratory findings to real-world production. With increased PHA production efficiency, the carbon footprint of PHA produced with ΔA3043/lipAB was reduced by 29.7 % compared to the original process using H16B, particularly in terms of energy consumption during production and waste generation in extraction per ton of PHA (Fig. 5C).

To explore further reduction of PHA production cost and carbon footprint, we tested waste cooking oil as an alternative feedstock in the 200-L fed-batch fermentation. Waste cooking oil primarily consists of fatty acids of varying chain lengths and saturation, originating from various plant and animal oils. Both H16B and ΔA3043/lipAB were able to consume waste cooking oil, but ΔA3043/lipAB exhibited superior performance, including higher oil consumption, DCW, PHA yield, and conversion rate. ΔA3043/lipAB produced a final yield of 194.3 g/L (94.9 % increase from H16B), with a conversion rate of 86.2 % (44.4 % increase from H16B) after 48 h fermentation (Fig. 5D and E). Projections (Table S5) indicated that replacing palm oil with waste cooking oil in ΔA3043/lipAB fermentation at 150 m^3 production scale could further reduce the carbon footprint by 39.0 %, resulting in a total reduction of 52.7 % compared to H16B production using palm oil (Fig. 5C).

Together, the engineered ΔA3043/lipAB strain demonstrated the robustness for cost-effective and sustainable PHA production using oil feedstocks including food-grade palm oil and crude waste cooking oil. Strategies and challenges for integrating waste cooking oil into industrial processes are further discussed in Discussion.

4. Discussion

The growing demand for sustainable bioplastics has placed PHA at the forefront of renewable material research. However, the high production costs associated with traditional carbon sources remain a significant bottleneck to industrial-scale adoption (Dong et al., 2023; Zytner et al., 2023). Our study addresses these challenges by engineering the industrial PHA production strain of *C. necator* to optimize the utilization efficiency of oil-based feedstocks, including both food-grade palm oil and waste cooking oil. While laboratory modifications can significantly enhance PHA yield, scaling up engineered strains often presents challenges that are not always addressed in the literature. In many studies, the focus is on laboratory-scale improvements, but issues encountered during the scale-up process are frequently overlooked. By resolving the scalability challenge with hypothesis-driven troubleshooting, our research offers innovative solutions for enhancing PHA yield, reducing production costs, and minimizing environmental impacts.

C. necator is naturally capable of utilizing a wide range of carbon sources, including oils, for PHA production, making it one of the most efficient strains for oil-based PHA production. However, its carbon source utilization efficiency remains suboptimal. As a naturally occurring strain, *C. necator* is constrained by complex regulatory networks that, while facilitating general carbon source utilization, limit its full potential for efficient oil consumption and PHA synthesis. The intricacy of these natural regulatory mechanisms makes rational design challenging, necessitating reliance on screening approaches for strain optimization. Through Tn-seq screening and adaptive evolution, we identified the *H16_A3043/H16_A3044* two-component system as a key regulator of oil consumption and PHA biosynthesis. The engineered strain ΔA3043 demonstrated enhanced β-oxidation activity, evidenced by increased acetyl-CoA levels and reduced palmityl-CoA and stearoyl-CoA levels, which directly improved PHA biosynthesis. The depletion of palmityl-CoA and stearoyl-CoA in ΔA3043 suggests that while β-oxidation is enhanced, fatty acid supply becomes limiting. In H16B, fatty acid uptake and β-oxidation are balanced, so lipAB overexpression does not improve oil utilization. However, in ΔA3043, the removal of H16_A3043 regulation accelerates β-oxidation, making lipid hydrolysis the bottleneck. This explains why lipAB overexpression enhances oil utilization only in ΔA3043, as it ensures a sufficient supply of free fatty acids for PHA biosynthesis. Upregulation of nucleotide biosynthesis pathways in ΔA3043 also contributed to faster cell growth during the logarithmic phase. However, transcriptomic analysis and experiments under phosphorus-free conditions revealed ΔA3043's impaired ability to sense environmental stress, highlighting a trade-off between enhanced metabolic activity and environmental adaptability. This limitation manifested in uncontrolled extracellular triglyceride accumulation, as the strain failed to regulate oil degradation into fatty acids effectively, which led to cell surface coverage and sludge formation during fermentation. We addressed this scalability issue by overexpressing the extracellular lipase lipAB, which successfully mitigated the sludge formation and enabled seamless scalability. While knocking out the two-component system significantly improved ΔA3043's palm oil-based PHA production, its regulatory mechanisms remain complex and are not fully understood. This system regulates numerous downstream genes involved in diverse metabolic pathways, suggesting untapped potential for targeted optimization that warrants future research to unravel these regulatory networks.

Scaling up ΔA3043/lipAB fermentation to 150 m^3 significantly improved oil consumption, PHA yield and conversion rate compared to H16B, demonstrating its robustness and compatibility with industrial-scale processes. The engineered strain achieved a final PHA yield of 264 g/L and a 25.4 % increase compared to H16B, with a conversion efficiency of 100 % after 60 h, the highest yield and conversion rate reported to the best of our knowledge (Arikawa and Matsumoto, 2016; Arikawa et al., 2017; Blunt et al., 2018; Arikawa and Sato, 2022). As the oil consumption rate maintained at relatively high levels at 60 h, extending the duration of fed-batch fermentation holds the potential of further increasing the PHA yield and conversion rate. Furthermore, replacing palm oil with waste cooking oil reduced the carbon footprint by 52.7 %, demonstrating the potential for coupling scalability with sustainability.

Beyond its lower carbon footprint, waste cooking oil also provides a cost-effective alternative to palm oil while maintaining high PHA yields and conversion rates. ΔA3043/lipAB achieved a final yield of 194.3 g/L and a conversion rate of 86.2 %, highlighting its potential for economic and sustainable production. However, the inherent variability in the composition of waste cooking oil, including undefined impurities and differences in fatty acid chain lengths and saturation, could influence microbial assimilation efficiency and PHA yield (Saratale et al., 2021; Getino et al., 2024). By contrast, palm oil's consistent quality supports predictable performance and higher yields. To enhance the feasibility of waste cooking oil for industrial applications, future research should focus on evaluating multiple batches and sources of waste cooking oil to better understand its impact on microbial metabolism and fermentation performance. Additionally, strategies such as pre-treating waste cooking oil to standardize its composition, engineering microbial strains to tolerate variability, or optimizing fermentation conditions could enhance its feasibility for industrial applications (Koller, 2018; Saratale et al., 2021). Last but not least, while waste cooking oil offers economic and environmental advantages, its integration into industrial processes requires careful consideration of government regulations and supply chain logistics.

Our study demonstrates the highest truly industrially viable PHA production yield reported to date. While numerous studies have explored PHA production, most were conducted at laboratory scale, with only a few reaching pilot-scale fermentation (≥50L). A detailed comparison (Table 2) shows that almost all pilot-scale studies reported

Table 2
Chronological summary of PHA yield for high-productivity fed-batch fermentation.

Microorganism	Carbon Source	Scale (L)	Biomass (g/L)	PHA yield (g/L)	Productivity (g/L/h)	DO ctrl[a]	Reference
Methylobacterium organophilum	methanol	2.5	250	130	1.86	$+O_2$	Kim et al. (1996)
Alcaligenes latus DSM 1123	sucrose	6.6	117	98	5.13	$+O_2$	Wang and Lee (1997a)
C. necator NCIMB 11599	glucose	60	281	232	3.14	?	Ryu et al. (1997)
E. coli XL1-Blue	glucose	6.6	204	157	3.20	$+O_2$	Wang and Lee (1997b)
		50	154	101	2.80		
E. coli XL1-Blue	glucose	6.6	194	142	4.63	?	Choi et al. (1998)
C. necator NCIMB 40124	rape Seed oil and propionic acid	15	204	137	2.11	Air	Naylor and Wood (1999)
C. necator NCIMB 11599	glucose	5	208	139	3.10	$+O_2$	Shang et al. (2003)
Bacillus megaterium	Molasses	90	85.3	40.1	1.67	Air	Kanjanachumpol et al. (2013)
C. necator	Palm oil	5	215	175	2.57	Air	Arikawa and Matsumoto (2016)
C. necator	Lipid particles[b]	10	?	217	4.52	Air	Takahashi et al. (2021)
C. necator	Palm oil	5	~220	196	2.88	Air	Arikawa and Sato (2022)
Halomonas lutescens	glucose	5	199	158	~4.5	Air	Shen et al. (2022)
C. necator	palm oil[c]	10	?	268	5.58	Air	Takahashi et al. (2023)
C. necator	palm oil	150 m^3	348	264	4.40	Air	This study

[a] Dissolved oxygen was enhanced using O_2-enriched air ($+O_2$) or Air.
[b] Palm oil fatty acid distillate was heated up tp 60.
[c] and sprayed into the culture liquid through 70C nozzle. c. The palm oil was refined through degumming, deacidification, decolorization, and deodorization, then emulsified by homogenized with water (6:4 ratio) at 60 °C with 0.5 % casein sodium as an emulsifier.

significantly lower PHA yields and productivities than ours, highlighting the challenge of achieving both high yield and high productivity at larger scales. Although one patent reported a slightly higher PHA yield (268 g/L) and a few studies achieved higher productivity, these approaches relied on pure oxygen supplementation or complex pre-treatment of palm oil, making them impractical for industrial production. In contrast, our process, which achieved 264 g/L PHA with a productivity of 4.40 g/L/h in 150 m^3 fed-batch fermentation, represents a scalable and economically feasible strategy for large-scale PHA manufacturing. By demonstrating high efficiency under realistic industrial conditions, our work lays a strong foundation for advancing PHA commercialization.

Beyond achieving high yields and productivity, ensuring PHA composition consistency at the industrial scale is crucial for successful commercialization. Our results demonstrate that both strain modifications and scale-up influence the molar composition of PHBH, particularly in terms of 3HHx incorporation (Fig. S9). The deletion of A3043 significantly increased 3HHx%, whereas lipAB overexpression had no notable effect in 500-mL fermentations. The 3HHx% increase in ΔA3043/lipAB compared to H16B was only 0.69 %, suggesting that this minor change is unlikely to have significant impact on polymer properties. During scale-up to 200 L, 15 m^3, and 150 m^3, 3HHx% fluctuated initially but stabilized at the largest scale (150 m^3), indicating that PHA composition remains predictable and reproducible in industrial fermentation. This suggests that while genetic modifications can fine-tune PHA monomer composition, the impact of fermentation scale on PHA composition is minor. In our study, the stability of 3HHx% at the industrial scale further supports the robustness and scalability of our fermentation process, reinforcing its suitability for large-scale PHA production with consistent material properties.

Future research should prioritize adaptive engineering to improve ΔA3043's resilience under fluctuating industrial conditions. Standardizing variable substrates like waste cooking oil through pre-treatment or bioprocess adjustments, conducting comprehensive life cycle and techno-economic analyses, and optimizing large-scale fermentation processes with real-time monitoring systems are essential next steps. Addressing these issues will unlock the full potential of oil-based substrates for sustainable PHA production, paving the way for cost-effective and environmentally friendly biopolymer solutions.

5. Conclusion

In conclusion, this study demonstrates the transformative potential of metabolic engineering in scalable and sustainable PHA production. By constructing *C. necator* ΔA3043/lipAB, we achieved significant enhancements in oil-based substrate utilization, improving PHA yield and conversion rate while substantially reducing the production carbon footprint. The strain's robust performance with alternative feedstocks, such as waste cooking oil, underscores its industrial viability and cost-effectiveness. Scaling up to the 150 m^3 fermentation system validated the feasibility of translating laboratory innovations into industrial-scale applications. Mechanistic insights into the *H16_A3043/H16_A3044* system uncovered critical regulatory mechanisms in substrate metabolism and stress response, paving the way for future strain optimizations. This work bridges critical gaps between experimental research and industrial implementation, offering a scalable, eco-friendly biopolymer solution to mitigate plastic pollution and advance global sustainability efforts.

CRediT authorship contribution statement

Tianyu Jiang: Methodology, Investigation. **Tingting Tan:** Validation, Investigation. **Zhiyuan Zong:** Investigation. **Dingding Fan:** Visualization, Software, Data curation. **Jianxin Wang:** Methodology, Investigation. **Yanci Qiu:** Investigation. **Xin Teng:** Writing – original draft, Visualization, Formal analysis. **Haoqian M. Zhang:** Writing – review & editing, Supervision. **Chitong Rao:** Writing – review & editing, Supervision, Conceptualization.

Funding

This work was funded by Bluepha Co., Ltd. STCSM grants 24QB2703700 and 2023PJD06.

Conflict of interest

Tianyu Jiang, Tingting Tan, Dingding Fan, Jianxin Wang, Yanci Qiu, Xin Teng, Haoqian M. Zhang, Chitong Rao are employees at Bluepha Co., Ltd.

Acknowledgement

We sincerely thank Dr. Li Chen and the Quantitative Metabolomics & Lipogenomics Platform of Institute of Metabolism & Integrative Biology, Fudan University for their invaluable assistance in conducting the metabolomics analysis. Their expertise and support were instrumental in advancing the findings of this study.

Appendix A. Supplementary data

Supplementary data to this article can be found online at https://doi.org/10.1016/j.ymben.2025.04.001.

Data availability

The RNA-seq raw data generated in this study are not publicly available due to commercial sensitivity. However, the analyzed RNA sequencing expression profiles, are provided in Table S6

References

Arikawa, H., Matsumoto, K., 2016. Evaluation of gene expression cassettes and production of poly(3-hydroxybutyrate-co-3-hydroxyhexanoate) with a fine modulated monomer composition by using it in Cupriavidus necator. Microb. Cell Fact. 15, 184.

Arikawa, H., Sato, S., 2022. Impact of various β-ketothiolase genes on PHBHHx production in Cupriavidus necator H16 derivatives. Appl. Microbiol. Biotechnol. 106, 3021–3032.

Arikawa, H., Matsumoto, K., Fujiki, T., 2017. Polyhydroxyalkanoate production from sucrose by Cupriavidus necator strains harboring csc genes from Escherichia coli W. Appl. Microbiol. Biotechnol. 101, 7497–7507.

Blunt, W., Levin, D.B., Cicek, N., 2018. Bioreactor operating strategies for improved polyhydroxyalkanoate (PHA) productivity. Polymers 10, 1197.

Braunegg, G., Bona, R., Koller, M., 2004. Sustainable Polymer Production. Polymer-Plastics Technology and Engineering.

Chen, S., Zhou, Y., Chen, Y., Gu, J., 2018. fastp: an ultra-fast all-in-one FASTQ preprocessor. Bioinformatics 34, i884–i890.

Chien Bong, C.P., Alam, M.N.H.Z., Samsudin, S.A., Jamaluddin, J., Adrus, N., Mohd Yusof, A.H., Muis, Z.A., Hashim, H., Salleh, M.M., Abdullah, A.R., Chuprat, B.R.B., 2021. A review on the potential of polyhydroxyalkanoates production from oil-based substrates. J. Environ. Manag. 298, 113461.

Choi, J.I., Lee, S.Y., Han, K., 1998. Cloning of the Alcaligenes latus polyhydroxyalkanoate biosynthesis genes and use of these genes for enhanced production of Poly(3-hydroxybutyrate) in Escherichia coli. Appl. Environ. Microbiol. 64, 4897–4903.

Cibulskis, K., Lawrence, M.S., Carter, S.L., Sivachenko, A., Jaffe, D., Sougnez, C., Gabriel, S., Meyerson, M., Lander, E.S., Getz, G., 2013. Sensitive detection of somatic point mutations in impure and heterogeneous cancer samples. Nat. Biotechnol. 31, 213–219.

Cingolani, P., Platts, A., Wang, L.L., Coon, M., Nguyen, T., Wang, L., Land, S.J., Lu, X., Ruden, D.M., 2012. A program for annotating and predicting the effects of single nucleotide polymorphisms. Fly 6, 80–92. SnpEff: SNPs in the genome of Drosophila melanogaster strain w1118; iso-2; iso-3.

DeJesus, M.A., Ambadipudi, C., Baker, R., Sassetti, C., Ioerger, T.R., 2015. TRANSIT - a software tool for Himar1 TnSeq analysis. PLoS Comput. Biol. 11, e1004401.

Dietrich, K., Dumont, M.-J., Del Rio, L.F., Orsat, V., 2019. Sustainable PHA production in integrated lignocellulose biorefineries. New Biotechnology 49, 161–168.

Dong, H., Yang, X., Shi, J., Xiao, C., Zhang, Y., 2023. Exploring the feasibility of cell-free synthesis as a platform for polyhydroxyalkanoate (PHA) production: opportunities and challenges. Polymers 15, 2333.

Dvořák, P., de Lorenzo, V., 2018. Refactoring the upper sugar metabolism of *Pseudomonas putida* for co-utilization of cellobiose, xylose, and glucose. Metab. Eng. 48, 94–108.

Getino, L., Martín, J.L., Chamizo-Ampudia, A., 2024. A review of polyhydroxyalkanoates: characterization, production, and application from waste. Microorganisms 12, 2028.

Gibson, D.G., Young, L., Chuang, R.-Y., Venter, J.C., Hutchison, C.A., Smith, H.O., 2009. Enzymatic assembly of DNA molecules up to several hundred kilobases. Nat. Methods 6, 343–345.

Insomphun, C., Mifune, J., Orita, I., Numata, K., Nakamura, S., Fukui, T., 2014. Modification of β-oxidation pathway in Ralstonia eutropha for production of poly(3-hydroxybutyrate-co-3-hydroxyhexanoate) from soybean oil. J. Biosci. Bioeng. 117, 184–190.

ISO 14040:2006. ISO, 2025. https://www.iso.org/standard/37456.html.

Jiang, G., Hill, D.J., Kowalczuk, M., Johnston, B., Adamus, G., Irorere, V., Radecka, I., 2016. Carbon sources for polyhydroxyalkanoates and an integrated biorefinery. Int. J. Mol. Sci. 17, 1157.

Johnson, K.R., Ellis, G., Toothill, C., 1977. The sulfophosphovanillin reaction for serum lipids: a reappraisal. Clin. Chem. 23, 1669–1678.

Kahar, P., Tsuge, T., Taguchi, K., Doi, Y., 2004. High yield production of polyhydroxyalkanoates from soybean oil by *Ralstonia eutropha* and its recombinant strain. Polym. Degrad. Stabil. 83, 79–86.

Kanjanachumpol, P., Kulpreecha, S., Tolieng, V., Thongchul, N., 2013. Enhancing polyhydroxybutyrate production from high cell density fed-batch fermentation of Bacillus megaterium BA-019. Bioproc. Biosyst. Eng. 36, 1463–1474.

Kim, S.W., Kim, P., Lee, H.S., Kim, J.H., 1996. High production of Poly-β-hydroxybutyrate (PHB) from Methylobacterium organophilum under potassium limitation. Biotechnol. Lett. 18, 25–30.

Kim, H.S., Oh, Y.H., Jang, Y.-A., Kang, K.H., David, Y., Yu, J.H., Song, B.K., Choi, J., Chang, Y.K., Joo, J.C., Park, S.J., 2016. Recombinant Ralstonia eutropha engineered to utilize xylose and its use for the production of poly(3-hydroxybutyrate) from sunflower stalk hydrolysate solution. Microb. Cell Fact. 15, 95.

Koller, M., 2018. A review on established and emerging fermentation schemes for microbial production of polyhydroxyalkanoate (PHA) biopolyesters. Fermentation 4, 30.

Koller, M., Braunegg, G., 2018. Advanced approaches to produce polyhydroxyalkanoate (PHA) biopolyesters in a sustainable and economic fashion. The EuroBiotech Journal 2, 89–103.

Koller, M., Hesse, P., Bona, R., Kutschera, C., Atlić, A., Braunegg, G., 2007. Potential of various archae- and eubacterial strains as industrial polyhydroxyalkanoate producers from whey. Macromol. Biosci. 7 (2), 218–226.

Kumar, V., Kumar, S., Singh, D., 2020. Microbial polyhydroxyalkanoates from extreme niches: bioprospection status, opportunities and challenges. Int. J. Biol. Macromol. 147, 1255–1267.

Le Meur, S., Zinn, M., Egli, T., Thöny-Meyer, L., Ren, Q., 2012. Production of medium-chain-length polyhydroxyalkanoates by sequential feeding of xylose and octanoic acid in engineered Pseudomonas putida KT2440. BMC Biotechnol. 12, 53.

Li, H., Durbin, R., 2009. Fast and accurate short read alignment with Burrows–Wheeler transform. Bioinformatics 25, 1754–1760.

Lim, S.W., Kansedo, J., Tan, I.S., Tan, Y.H., Nandong, J., Lam, M.K., Ongkudon, C.M., 2023. Microbial valorization of oil-based substrates for polyhydroxyalkanoates (PHA) production – current strategies, status, and perspectives. Process Biochem. 130, 715–733.

Love, M.I., Huber, W., Anders, S., 2014. Moderated estimation of fold change and dispersion for RNA-seq data with DESeq2. Genome Biol. 15, 550.

Martin, M., 2011. Cutadapt removes adapter sequences from high-throughput sequencing reads. EMBnet.journal. 17, 10–12.

Naylor, L.A., Wood, J.C., 1999. Process for the Microbiological Production of Pha-Polymers.

Nielsen, C., Rahman, A., Rehman, A.U., Walsh, M.K., Miller, C.D., 2017. Food Waste Conversion to Microbial Polyhydroxyalkanoates. Microbial Biotechnology 10, 1338–1352.

Ng, K.-S., Ooi, W.-Y., Goh, L.-K., Shenbagarathai, R., Sudesh, K., 2010. Evaluation of jatropha oil to produce poly(3-hydroxybutyrate) by *Cupriavidus necator* H16. *Polymer Degradation and Stability*. International Conference on Bio-based Polymers (ICBP 2009) "Ensuring A Sustainable Tomorrow." 95, 1365–1369.

Orita, I., Iwazawa, R., Nakamura, S., Fukui, T., 2012. Identification of mutation points in *Cupriavidus necator* NCIMB 11599 and genetic reconstitution of glucose-utilization ability in wild strain H16 for polyhydroxyalkanoate production. J. Biosci. Bioeng. 113, 63–69.

Park, S.J., Choi, J., Lee, S.Y., 2005. Engineering of *Escherichia coli* fatty acid metabolism for the production of polyhydroxyalkanoates. Enzym. Microb. Technol. 36, 579–588.

Park, H., He, H., Yan, X., Liu, X., Scrutton, N.S., Chen, G.-Q., 2024. PHA is not just a bioplastic. Biotechnol. Adv. 71, 108320.

Patro, R., Duggal, G., Love, M.I., Irizarry, R.A., Kingsford, C., 2017. Salmon provides fast and bias-aware quantification of transcript expression. Nat. Methods 14, 417–419.

Picard tools - by Broad Institute. https://broadinstitute.github.io/picard/, 2024.

Quelas, J.I., Cabrera, J.J., Díaz-Peña, R., Sánchez-Schneider, L., Jiménez-Leiva, A., Tortosa, G., Delgado, M.J., Pettinari, M.J., Lodeiro, A.R., del Val, C., Mesa, S., 2024. Pleiotropic effects of PhaR regulator in Bradyrhizobium diazoefficiens microaerobic metabolism. Int. J. Mol. Sci. 25, 2157.

Raberg, M., Reinecke, F., Reichelt, R., Malkus, U., König, S., Pötter, M., Fricke, W.F., Pohlmann, A., Voigt, B., Hecker, M., Friedrich, B., Bowien, B., Steinbüchel, A., 2008. Ralstonia eutropha H16 flagellation changes according to nutrient supply and state of poly(3-hydroxybutyrate) accumulation. Appl. Environ. Microbiol. 74, 4477–4490.

Rao, U., Sridhar, R., Sehgal, P.K., 2010. Biosynthesis and biocompatibility of poly(3-hydroxybutyrate-co-4-hydroxybutyrate) produced by *Cupriavidus necator* from spent palm oil. Biochem. Eng. J. 49, 13–20.

Reinecke, F., Steinbüchel, A., 2009. Ralstonia eutropha strain H16 as model organism for PHA metabolism and for biotechnological production of technically interesting biopolymers. J. Mol. Microbiol. Biotechnol. 16, 91–108.

Ruiz, C., Kenny, S.T., Narancic, T., Babu, R., Connor, K.O., 2019. Conversion of waste cooking oil into medium chain polyhydroxyalkanoates in a high cell density fermentation. J. Biotechnol. 306, 9–15.

Ryu, H.W., Hahn, S.K., Chang, Y.K., Chang, H.N., 1997. Production of poly(3-hydroxybutyrate) by high cell density fed-batch culture of Alcaligenes eutrophus with phospate limitation. Biotechnol. Bioeng. 55, 28–32.

Saratale, R.G., Cho, S.-K., Saratale, G.D., Kumar, M., Bharagava, R.N., Varjani, S., Kadam, A.A., Ghodake, G.S., Palem, R.R., Mulla, S.I., Kim, D.-S., Shin, H.-S., 2021. An overview of recent advancements in microbial polyhydroxyalkanoates (PHA) production from dark fermentation acidogenic effluents: a path to an integrated bio-refinery. Polymers 13, 4297.

Saravanan, K., Umesh, M., Kathirvel, P., 2022. Microbial polyhydroxyalkanoates (PHAs): a review on biosynthesis, properties, fermentation strategies and its prospective applications for sustainable future. J. Polym. Environ. 30, 4903–4935.

Shang, L., Jiang, M., Chang, H.N., 2003. Poly(3-hydroxybutyrate) synthesis in fed-batch culture of Ralstonia eutropha with phosphate limitation under different glucose concentrations. Biotechnol. Lett. 25, 1415–1419.
Shen, Hongwei, Lv, Jinyan, Yin, Huijuan, Si, Tuwei, Yu, Liusong, He, Shiqi, 2022. A Strain of Halomonas and its Application. CN113801810B[P].
Sheu, D.-S., Lee, C.-Y., 2004. Altering the substrate specificity of polyhydroxyalkanoate synthase 1 derived from Pseudomonas putida GPo1 by localized semirandom mutagenesis. J. Bacteriol. 186, 4177–4184.
Siegel, E.C., Bryson, V., 1967. Mutator gene of Escherichia coli B. J. Bacteriol. 94, 38–47.
Simon, R., Priefer, U., Pühler, A., 1983. A Broad host range mobilization system for in vivo genetic engineering: transposon mutagenesis in gram negative bacteria. Nat. Biotechnol. 1, 784–791.
Takahashi, Togari, Shiohomi, Nishimori, Yu, Hirano, Hiroaki, Ichiriki, Akihisa, Kanda, 2021. Method for Producing Lipid Particles in Liquid and Method for Culturing Microorganisms. WO2021106462A1[P].
Takahashi, Togari, Li, Wangyin, Shingo, Kobayashi, 2023. Method for Producing Polyhydroxyalkanoates. JP2020522177A[P].
Tang, R., Weng, C., Peng, X., Han, Y., 2020. Metabolic engineering of Cupriavidus necator H16 for improved chemoautotrophic growth and PHB production under oxygen-limiting conditions. Metab. Eng. 61, 11–23.
Wang, F., Lee, S.Y., 1997a. Poly(3-Hydroxybutyrate) production with high productivity and high polymer content by a fed-batch culture of alcaligenes latus under nitrogen limitation. Appl. Environ. Microbiol. 63, 3703–3706.
Wang, F., Lee, S.Y., 1997b. Production of poly(3-hydroxybutyrate) by fed-batch culture of filamentation-suppressed recombinant Escherichia coli. Appl. Environ. Microbiol. 63, 4765–4769.
Wang, J., Liu, S., Huang, J., Cui, R., Xu, Y., Song, Z., 2023. Genetic engineering strategies for sustainable polyhydroxyalkanoate (PHA) production from carbon-rich wastes. Environ. Technol. Innovat. 30, 103069.
Wernet, G., Bauer, C., Steubing, B., Reinhard, J., Moreno-Ruiz, E., Weidema, B., 2016. The ecoinvent database version 3 (part I): overview and methodology. Int. J. Life Cycle Assess. 21, 1218–1230.
Wu, T., Hu, E., Xu, S., Chen, M., Guo, P., Dai, Z., Feng, T., Zhou, L., Tang, W., Zhan, L., Fu, X., Liu, S., Bo, X., Yu, G., 2021. clusterProfiler 4.0: a universal enrichment tool for interpreting omics data. Innovation 2.
Xin, F., Yan, W., Zhou, J., Wu, H., Dong, W., Ma, J., Zhang, W., Jiang, M., 2018. Exploitation of novel wild type solventogenic strains for butanol production. Biotechnol. Biofuels 11.
Yañez, L., Conejeros, R., Vergara-Fernández, A., Scott, F., 2020. Beyond intracellular accumulation of polyhydroxyalkanoates: chiral hydroxyalkanoic acids and polymer secretion. Front. Bioeng. Biotechnol. 8.
Yin, J., Wang, Y., Li, J., Hou, J., Zou, L., Chen, Z., 2023. Engineered Microorganism Expressing Acetoacetyl Coenzyme a Reductase Variant and Method for Increasing Proportion of 3-hydroxyhexanoic Acid in Pha. WO2023193352A1 [P].
Zhgun, A.A., 2023. Industrial production of antibiotics in fungi: current state, deciphering the molecular basis of classical strain improvement and increasing the production of high-yielding strains by the addition of low-molecular weight inducers. Fermentation 9, 1027.
Zytner, P., Kumar, D., Elsayed, A., Mohanty, A., Ramarao, B.V., Misra, M., 2023. A review on polyhydroxyalkanoate (PHA) production through the use of lignocellulosic biomass. RSC Sustain. 1, 2120–2134.